

The recoil correction and spin-orbit force for the possible $B^*\bar{B}^*$ and $D^*\bar{D}^*$ states

Lu Zhao^{1*}, Li Ma^{1†}, Shi-Lin Zhu^{1,2‡}

¹ Department of Physics and State Key Laboratory of Nuclear Physics and Technology, Peking University, Beijing 100871, China

² Collaborative Innovation Center of Quantum Matter, Beijing 100871, China

In the framework of the one-boson exchange model, we have calculated the effective potentials between two heavy mesons $B^*\bar{B}^*$ and $D^*\bar{D}^*$ from the t - and u -channel π -, η -, ρ -, ω - and σ -meson exchanges. We keep the recoil corrections to the $B^*\bar{B}^*$ and $D^*\bar{D}^*$ systems up to $O(\frac{1}{M^2})$, which turns out to be important for the very loosely bound molecular states. Our numerical results show that the momentum-related corrections are favorable to the formation of the molecular states in the $I^G = 1^+$, $J^{PC} = 1^{+-}$ in the $B^*\bar{B}^*$ and $D^*\bar{D}^*$ systems.

PACS numbers: 13.75.-n, 13.75.Cs, 14.20.Gk

I. INTRODUCTION

A lot of charmonium-like states have been reported in the past decade by the experiment collaborations such as Belle, *Barbar*, CDF, D0, LHCb, BESIII, and CLEOc. The underlying structures of many charmonium-like states are not very clear. Sometimes they are called as XYZ states. They decay into conventional chromium, but not all of them can be accommodated into the quark-model charmonium spectrum. The neutral XYZ states include $X(3872)$ [1], $Y(4260)$ [2], $Y(4008)$ [3], $Y(4360)$ [4], $Y(4660)$ [5], and $Y(4630)$ [6] etc. There are also many charged charmonium-like states such as $Z_1(4050)$ and $Z_2(4250)$ [7], $Z_c(4485)$ [8, 9], $Z_c(3900)$ [10–12], $Z_c(4020)$ [13], $Z_c(4025)$ [14]. The charged bottomonium-like states $Z_b(10610)$ and $Z_b(10650)$ were observed by Belle Collaboration [15].

Theoretical speculations of these XYZ states include the hybrid meson [16], tetraquark states [17–23], dynamically generated resonance [24] and molecular states [25–33] etc. Since many of these XYZ states are close to the thresholds of a pair of charmed or bottom mesons, the molecular hypothesis seems a natural picture for some of these states.

Within the framework of the molecular states, there exist extensive investigations of the charged Z_c and Z_b states [34–44]. In our previous work [45], we explored the possibility of $Z_c(3900)$ as the isovector molecule partner of $X(3872)$ and considered the recoil correction and the spin-orbit force in the $D\bar{D}^*$ and $B\bar{B}^*$ system very carefully.

Although there exist quite a few literatures on the possibility of $Z_c(4025)$ as the $D^*\bar{D}^*$ molecular state and $Z_b(10650)$ as the $B^*\bar{B}^*$ molecular state, most of the available investigations are either based on the heavy quark spin-flavor symmetry or derived in the $m_Q \rightarrow \infty$. In other words, the recoil correction and the spin-orbit interaction have not been investigated for the $D^*\bar{D}^*$ and $B^*\bar{B}^*$ systems. Since the binding energies of these system are very small, the high order recoil correction and the spin-orbit interaction may lead to significant corrections.

In this work, we will go one step further. We will consider the recoil correction and the spin-orbit force for the $D^*\bar{D}^*$ and $B^*\bar{B}^*$ systems. With the one-boson-exchange model (OBE), we will derive the effective potential with the relativistic Lagrangian and keep the momentum related terms explicitly in order to derive the recoil correction and the spin-orbit interaction up to $O(1/M^2)$, where M is the mass of the heavy meson. We investigate the $B^*\bar{B}^*$ system with $I^G = 1^+$, $J^P = 1^{+-}$ for $Z_b(10650)$, and the $D^*\bar{D}^*$ system with $I^G = 1^+$, $J^P = 1^{+-}$ for $Z_c(4025)$. For completeness, we also investigate the $B^*\bar{B}^*$ system and $D^*\bar{D}^*$ system with other quantum numbers: $I^G = 1^-$, $J^P = 1^{++}$, $I^G = 0^+$, $J^P = 1^{++}$, and $I^G = 0^-$, $J^P = 1^{+-}$. Compared to the $D\bar{D}^*$ case, the expressions of the recoil corrections and spin orbit force are more complicated. There appear several new structures. For some systems, the numerical results show that the high order correction is important for the loosely bound heavy-meson states.

This paper is organized as follows. We first introduce the formalism of the derivation of the effective potential in Sec. II. We present our numerical results in Sec. III and Sec. IV. The last section is the summary and discussion.

II. THE EFFECTIVE POTENTIAL

A. Wave function, Effective Lagrangian and Coupling constants

First, we construct the flavor wave functions of the isovector and isoscalar molecular states composed of the $B^*\bar{B}^*$ and $D^*\bar{D}^*$ as in Refs. [36, 37]. The flavor wave function of the $B^*\bar{B}^*$ system reads

$$\begin{cases} |1, 1\rangle = |B^{*+}\bar{B}^{*0}\rangle, \\ |1, -1\rangle = |B^{*-}\bar{B}^{*0}\rangle, \\ |1, 0\rangle = \frac{1}{\sqrt{2}}(|B^{*+}\bar{B}^{*-}\rangle - |B^{*0}\bar{B}^{*0}\rangle), \end{cases} \quad (1)$$

$$|0, 0\rangle = \frac{1}{\sqrt{2}}(|B^{*+}\bar{B}^{*-}\rangle + |B^{*0}\bar{B}^{*0}\rangle) \quad (2)$$

For the $D^*\bar{D}^*$ system

$$\begin{cases} |1, 1\rangle = |\bar{D}^{*0}D^{*+}\rangle, \\ |1, -1\rangle = |\bar{D}^{*0}D^{*-}\rangle, \\ |1, 0\rangle = \frac{1}{\sqrt{2}}(|\bar{D}^{*0}D^{*0}\rangle - |\bar{D}^{*-}D^{*+}\rangle), \end{cases} \quad (3)$$

*Email: Luzhao@pku.edu.cn

†Email: lima@pku.edu.cn

‡Email: zhushl@pku.edu.cn

$$|0, 0\rangle = \frac{1}{\sqrt{2}}(|\bar{D}^{*0} D^{*0}\rangle + |D^{*-} D^{*+}\rangle) \quad (4)$$

The meson exchange Feynman diagrams for the $B^* \bar{B}^*$ and $D^* \bar{D}^*$ systems at the tree level is shown in Fig. 1.

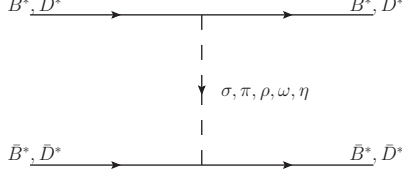


FIG. 1: The Feynman diagrams for both the $D^* \bar{D}^*$ and $B^* \bar{B}^*$ systems at the tree level.

Based on the chiral symmetry, the Lagrangian for the pseudoscalar, scalar and vector meson interaction with the heavy flavor mesons reads

$$\begin{aligned} \mathcal{L}_P = & -i \frac{2g}{f_\pi} \bar{M} P_b^{*\mu} \partial_\mu \phi_{ba} P_a^\dagger + i \frac{2g}{f_\pi} \bar{M} P_b \partial_\mu \phi_{ba} P_a^{*\mu\dagger} \\ & - \frac{g}{f_\pi} P_b^{*\mu} \partial^\alpha \phi_{ba} \partial^\beta P_a^{*\nu\dagger} \epsilon_{\mu\nu\alpha\beta} + \frac{g}{f_\pi} \partial^\beta P_b^{*\mu} \partial^\alpha \phi_{ba} P_a^{*\nu\dagger} \epsilon_{\mu\nu\alpha\beta} \end{aligned} \quad (5)$$

$$\begin{aligned} \widetilde{\mathcal{L}}_P = & -i \frac{2g}{f_\pi} \widetilde{M} P_a^{*\mu} \partial_\mu \phi_{ab} \widetilde{P}_b^\dagger - i \frac{2g}{f_\pi} \widetilde{M} P_a^{*\mu\dagger} \partial_\mu \phi_{ab} \widetilde{P}_b \\ & + \frac{g}{f_\pi} \partial^\beta P_a^{*\mu\dagger} \partial^\alpha \phi_{ab} \widetilde{P}_b^{*\nu} \epsilon_{\mu\nu\alpha\beta} - \frac{g}{f_\pi} \widetilde{P}_a^{*\mu\dagger} \partial^\alpha \phi_{ab} \partial^\beta \widetilde{P}_b^{*\nu} \epsilon_{\mu\nu\alpha\beta} \end{aligned} \quad (6)$$

$$\begin{aligned} \mathcal{L}_V = & i \frac{\beta g_v}{\sqrt{2}} P_b V_{ba}^\mu \partial_\mu P_a^\dagger - i \frac{\beta g_v}{\sqrt{2}} \partial_\mu P_b V_{ba}^\mu P_a^\dagger \\ & - i \sqrt{2} \lambda g_v \epsilon_{\mu\alpha\beta\nu} \partial^\mu P_b \partial^\alpha V_{ba}^\beta P_a^{*\nu\dagger} \\ & - i \sqrt{2} \lambda g_v \epsilon_{\mu\alpha\beta\nu} P_b^{*\mu} \partial^\alpha V_{ba}^\beta \partial^\nu P_a^\dagger \\ & - i \frac{\beta g_v}{\sqrt{2}} P_b^{*\nu} V_{ba}^\mu \partial_\mu P_a^{*\dagger} + i \frac{\beta g_v}{\sqrt{2}} \partial_\mu P_b^{*\nu} V_{ba}^\mu P_a^{*\dagger} \\ & - i 2 \sqrt{2} \lambda g_v \bar{M}^* P_b^{*\mu} (\partial_\mu V_\nu - \partial_\nu V_\mu)_{ba} P_a^{*\nu\dagger}, \end{aligned} \quad (7)$$

$$\begin{aligned} \widetilde{\mathcal{L}}_V = & -i \frac{\beta g_v}{\sqrt{2}} \partial_\mu \widetilde{P}_a^\dagger V_{ab}^\mu \widetilde{P}_b + i \frac{\beta g_v}{\sqrt{2}} \widetilde{P}_a^\dagger V_{ab}^\mu \partial_\mu \widetilde{P}_b \\ & + i \sqrt{2} \lambda g_v \epsilon_{\mu\alpha\beta\nu} \widetilde{P}_a^{*\mu\dagger} \partial^\alpha V_{ab}^\beta \partial^\nu \widetilde{P}_b \\ & + i \sqrt{2} \lambda g_v \epsilon_{\mu\alpha\beta\nu} \partial^\mu \widetilde{P}_a^\dagger \partial^\alpha V_{ab}^\beta \widetilde{P}_b^{*\nu} \\ & + i \frac{\beta g_v}{\sqrt{2}} \partial_\mu \widetilde{P}_a^{*\dagger} V_{ba}^\mu \widetilde{P}_b^{*\nu} - i \frac{\beta g_v}{\sqrt{2}} \widetilde{P}_a^{*\dagger} V_{ba}^\mu \partial_\mu \widetilde{P}_b^{*\nu} \\ & - i 2 \sqrt{2} \lambda g_v \bar{M}^* \widetilde{P}_a^{*\mu\dagger} (\partial_\mu V_\nu - \partial_\nu V_\mu)_{ab} \widetilde{P}_b^{*\nu}, \end{aligned} \quad (8)$$

$$\mathcal{L}_S = -2g_s \bar{M} P_b \sigma P_b^\dagger + 2g_s \bar{M}^* P_b^{*\mu} \sigma P_{\mu b}^{*\dagger} \quad (9)$$

$$\widetilde{\mathcal{L}}_S = -2g_s \bar{M} P_a^\dagger \sigma \widetilde{P}_a + 2g_s \bar{M}^* P_{\mu a}^{*\dagger} \sigma \widetilde{P}_a^{*\mu} \quad (10)$$

where the heavy flavor meson fields P and P^* represent $P = (D^0, D^+)$ or (B^-, \bar{B}^0) and $P^* = (D^{*0}, D^{*+})$ or (B^{*-}, \bar{B}^{*0}) . Its corresponding heavy anti-meson fields \bar{P} and \bar{P}^* represent $\bar{P} = (\bar{D}^0, D^-)$ or (B^+, B^0) and $\bar{P}^* = (\bar{D}^{*0}, D^{*-})$ or (B^{*+}, B^{*0}) . ϕ , V represent the the exchanged pseudoscalar and vector meson matrices. σ is the only scalar meson interacting with the heavy flavor meson.

$$\phi = \begin{pmatrix} \frac{\pi^0}{\sqrt{2}} + \frac{\eta}{\sqrt{6}} & \pi^+ \\ \pi^- & -\frac{\pi^0}{\sqrt{2}} + \frac{\eta}{\sqrt{6}} \end{pmatrix} \quad (11)$$

$$V = \begin{pmatrix} \frac{\rho^0}{\sqrt{2}} + \frac{\omega}{\sqrt{2}} & \rho^+ \\ \rho^- & -\frac{\rho^0}{\sqrt{2}} + \frac{\omega}{\sqrt{2}} \end{pmatrix} \quad (12)$$

According to the OBE model, five mesons (π , σ , ρ , ω and η) contribute to the effective potential. For the $D^* \bar{D}^*$ and $B^* \bar{B}^*$ systems, the potentials are the same for the three isovector states in Eqs. (1)~(4) with the exact isospin symmetry. Expanding the Lagrangian densities in Eqs. (5)~(10) leads to each meson's contribution for this channel. These channel-dependent coefficients are listed in Table I.

The pionic coupling constant $g = 0.59$ is extracted from the width of D^{*+} [46]. $f_\pi = 132$ MeV is the pion decay constant. According the vector meson dominance mechanism, the parameters g_v and β can be determined as $g_v = 5.8$ and $\beta = 0.9$. At the same time, by matching the form factor obtained from the light cone sum rule and that calculated from the lattice QCD, we can get $\lambda = 0.56 \text{ GeV}^{-1}$ [47, 48]. The coupling constant related to the scalar meson exchange is $g_s = g_\pi/2 \sqrt{6}$ with $g_\pi = 3.73$ [37, 49]. All these parameters are listed in Table II.

TABLE I: coefficients

	isospin	meson-exchange				
		ρ	ω	σ	π	η
$D^* \bar{D}^*$	$I = 1$	-1/2	1/2	1	-1/2	1/6
	$I = 0$	3/2	1/2	1	3/2	1/6
$B^* \bar{B}^*$	$I = 1$	-1/2	1/2	1	-1/2	1/6
	$I = 0$	3/2	1/2	1	3/2	1/6

In order to include all the momentum-related terms in our calculation, we introduce the polarization vector of the vector mesons. At the rest frame we have

$$\epsilon_\lambda = (0, \vec{\epsilon}_\lambda) \quad (13)$$

We make a lorentz boost to Eq. 13 to derive the polarization vector in the laboratory frame

$$\epsilon_\lambda^{lab} = \left(\frac{\vec{p} \cdot \vec{\epsilon}_\lambda}{m}, \vec{\epsilon}_\lambda + \frac{\vec{p}(\vec{p} \cdot \vec{\epsilon}_\lambda)}{m(P_0 + m)} \right) \quad (14)$$

TABLE II: The coupling constants and masses of the heavy mesons and the exchanged light mesons used in our calculation. The masses of the mesons are taken from the PDG [50]

	mass(MeV)	coupling constants
pseudoscalar	$m_\pi = 134.98$	$g = 0.59$
	$m_\eta = 547.85$	$f_\pi = 132 MeV$
vector	$m_\rho = 775.49$	$g_v = 5.8$
	$m_\omega = 782.65$	$\beta = 0.9$ $\lambda = 0.56 GeV^{-1}$
scalar	$m_\sigma = 600$	$g_s = g_\pi/2\sqrt{6}$ $g_\pi = 3.73$
heavy flavor	$m_{D^*} = 2010.25$	
	$m_{B^*} = 5325.0$	

where $p = (p_0, \mathbf{p})$ is the particle's 4-momentum in the laboratory frame and m is the mass of the particle.

B. Effective potential

With the wave function and Feynman diagram, we can derive the relativistic scattering amplitude at the tree level

$$\langle f|S|i\rangle = \delta_{fi} + i\langle f|T|i\rangle = \delta_{fi} + (2\pi)^4 \delta^4(p_f - p_i) iM_{fi}, \quad (15)$$

where the T-matrix is the interaction part of the S-matrix and M_{fi} is defined as the invariant matrix element. After applying Bonn approximation to the Lippmann-Schwinger equation, the S-matrix reads

$$\langle f|S|i\rangle = \delta_{fi} - 2\pi\delta(E_f - E_i) iV_{fi} \quad (16)$$

with V_{fi} being the effective potential. Considering the different normalization conventions used for the scattering amplitude M_{fi} , T-matrix T_{fi} and V_{fi} , we have

$$V_{fi} = -\frac{M_{fi}}{\sqrt{\prod_f 2p_f^0} \prod_i 2p_i^0} \approx -\frac{M_{fi}}{\sqrt{\prod_f 2m_f^0} \prod_i 2m_i^0} \quad (17)$$

where $p_{f(i)}$ denotes the four momentum of the final (initial) state.

During our calculation, $P_1 = (E_1, \vec{p})$ and $P_2 = (E_2, -\vec{p})$ denote the four momenta of the initial states in the center mass system, while $P_3 = (E_3, \vec{p}')$ and $P_4 = (E_4, -\vec{p}')$ denote the four momenta of the final states, respectively.

$$q = P_3 - P_1 = (E_3 - E_1, \vec{p}' - \vec{p}) = (E_2 - E_4, \vec{q}) \quad (18)$$

is the transferred four momentum or the four momentum of the meson propagator. For convenience, we always use

$$\vec{q} = \vec{p}' - \vec{p} \quad (19)$$

and

$$\vec{k} = \frac{1}{2}(\vec{p}' + \vec{p}) \quad (20)$$

instead of \vec{p}' and \vec{p} in the practical calculation.

In the OBE model, a form factor is introduced at each vertex to suppress the high momentum contribution. We take the conventional form for the form factor as in the Bonn potential model.

$$F(q) = \frac{\Lambda^2 - m_\alpha^2}{\Lambda^2 - q^2} = \frac{\Lambda^2 - m_\alpha^2}{\Lambda^2 + \vec{q}^2} \quad (21)$$

m_α is the mass of the exchanged meson and m^* is the mass of the heavy flavor meson D^* or B^* . So far, the effective potential is derived in the momentum space. In order to solve the time independent Schrödinger equation in the coordinate space, we need to make the Fourier transformation to $V(\vec{q}, \vec{k})$. The details of the Fourier transformations are presented in the Appendix.

The expressions of the potential through exchanging the σ , ρ mesons are

$$\begin{aligned} V_\sigma = & -C_\sigma g_s^2 (\vec{\epsilon}_b \cdot \vec{\epsilon}_a^\dagger)(\vec{\epsilon}_{b'} \cdot \vec{\epsilon}_{a'}^\dagger) F_{1\sigma} \\ & -C_\sigma g_s^2 \frac{1}{m^{*2}} [(\vec{\epsilon}_b \cdot \vec{\epsilon}_a^\dagger)(\vec{\epsilon}_{b'} \cdot \vec{\epsilon}_{a'}^\dagger) F_{3t1\sigma} + S'_{12} F_{3t2\sigma}] \\ & +C_\sigma g_s^2 \frac{1}{m^{*2}} i(\vec{\epsilon}_{b'} \cdot \vec{\epsilon}_{a'}^\dagger)[(\vec{\epsilon}_a^\dagger \times \vec{\epsilon}_b) \cdot \vec{L}] F_{5t\sigma} \end{aligned} \quad (22)$$

$$\begin{aligned} V_\rho = & -C_\rho \frac{\beta^2 g_v^2}{2} (\vec{\epsilon}_b \cdot \vec{\epsilon}_a^\dagger)(\vec{\epsilon}_{b'} \cdot \vec{\epsilon}_{a'}^\dagger) F_{1\rho} \\ & -C_\rho 2\lambda^2 g_v^2 (\vec{\epsilon}_b \times \vec{\epsilon}_a^\dagger)(\vec{\epsilon}_{b'} \times \vec{\epsilon}_{a'}^\dagger) F_{2\rho} \\ & +C_\rho 2\lambda^2 g_v^2 [(\vec{\epsilon}_b \times \vec{\epsilon}_a^\dagger)(\vec{\epsilon}_{b'} \times \vec{\epsilon}_{a'}^\dagger) F_{3t1\rho} + \tilde{S}_{12} F_{3t2\rho}] \\ & -C_\rho (\frac{\beta^2 g_v^2}{2m^{*2}} - \frac{2\lambda\beta g_v^2}{m^*}) [(\vec{\epsilon}_b \cdot \vec{\epsilon}_a^\dagger)(\vec{\epsilon}_{b'} \cdot \vec{\epsilon}_{a'}^\dagger) F_{3t1\rho} + S'_{12} F_{3t2\rho}] \\ & -C_\rho \frac{\beta^2 g_v^2}{2m^{*2}} (\vec{\epsilon}_b \cdot \vec{\epsilon}_a^\dagger)(\vec{\epsilon}_{b'} \cdot \vec{\epsilon}_{a'}^\dagger) [F_{4t1\rho} + \{-\frac{1}{2}\nabla^2, F_{4t2\rho}\}] \\ & +C_\rho (\frac{\beta^2 g_v^2}{2m^{*2}} - \frac{4\lambda\beta g_v^2}{m^*}) i(\vec{\epsilon}_{b'} \cdot \vec{\epsilon}_{a'}^\dagger)[(\vec{\epsilon}_a^\dagger \times \vec{\epsilon}_b) \cdot \vec{L}] F_{5t\rho} \end{aligned} \quad (23)$$

The ω and ρ meson exchange potentials have the same form except that the meson mass and channel-dependent coefficients are different.

The expression of the potential through exchanging the π meson is

$$V_\pi = C_\pi \frac{g_\pi^2}{f_\pi^2} [(\vec{\epsilon}_b \times \vec{\epsilon}_a^\dagger)(\vec{\epsilon}_{b'} \times \vec{\epsilon}_{a'}^\dagger) F_{3t1\pi} + \tilde{S}_{12} F_{3t2\pi}] \quad (24)$$

where S'_{12} and \tilde{S}_{12} have the form

$$S'_{12} = [3(\vec{r} \cdot \vec{\epsilon}_b)(\vec{r} \cdot \vec{\epsilon}_a^\dagger) - (\vec{\epsilon}_b \cdot \vec{\epsilon}_a^\dagger)](\vec{\epsilon}_{b'} \cdot \vec{\epsilon}_{a'}^\dagger) \quad (25)$$

$$\tilde{S}_{12} = 3[\vec{r} \cdot (\vec{\epsilon}_b \times \vec{\epsilon}_a^\dagger)][\vec{r} \times (\vec{\epsilon}_{b'} \cdot \vec{\epsilon}_{a'}^\dagger)] - (\vec{\epsilon}_b \times \vec{\epsilon}_a^\dagger)(\vec{\epsilon}_{b'} \times \vec{\epsilon}_{a'}^\dagger) \quad (26)$$

Compared to the $D\bar{D}^*$ case, there appear several new interaction operators: $(\vec{\epsilon}_b \times \vec{\epsilon}_a^\dagger)(\vec{\epsilon}_{b'} \times \vec{\epsilon}_{a'}^\dagger)$, S'_{12} , \tilde{S}_{12} and $i(\vec{\epsilon}_{b'} \cdot \vec{\epsilon}_a^\dagger)[(\vec{\epsilon}_a^\dagger \times \vec{\epsilon}_b) \cdot \vec{L}]$. These operators represent the new form of the tensor, spin-spin and spin-orbit interactions.

Similarly, the η and π meson exchange potential has the same form in the $D^*\bar{D}^*$ and $B^*\bar{B}^*$ system except the meson mass and channel-dependent coefficients. The explicit forms of $\mathcal{F}_{\mu\alpha}, \mathcal{F}_{\mu\alpha\alpha}, \mathcal{F}_{\mu\nu\alpha}, \mathcal{F}_{\mu\nu\alpha\alpha}$ are shown in the Appendix.

In our calculation, we explicitly consider the external momentum of the initial and final states. Due to the recoil corrections, several new terms appear which were omitted in the heavy quark symmetry limit. These momentum dependent terms are related to the momentum $\vec{k} = \frac{1}{2}(\vec{p}' + \vec{p})$:

$$\frac{\vec{k}^2}{\vec{q}^2 + m_\alpha^2} \quad (27)$$

and

$$\frac{i(\vec{\epsilon}_{b'} \cdot \vec{\epsilon}_{a'}^\dagger)[(\vec{\epsilon}_a^\dagger \times \vec{\epsilon}_b) \cdot (\vec{k} \times \vec{q})]}{\vec{q}^2 + m_\alpha^2} \quad (28)$$

The term in Eq. (28) is the well-known spin orbit force. In short, all the terms in the effective potentials in the form of $F_{3t1\rho}, F_{4t1\rho}, F_{5t\rho}$ etc with the sub-indices 3, 4, 5 arise from the recoil corrections and vanish when the heavy meson mass m^* goes to infinity. The recoil correction and the spin orbit force appear at $O(1/M^2)$.

C. Schrödinger equation

With the effective potential $V(\vec{r})$ in Eqs. (23) ~ (27), we are able to study the binding property of the system by solving the Schrödinger Equation

$$(-\frac{\hbar^2}{2\mu}\nabla^2 + V(\vec{r}) - E)\Psi(\vec{r}) = 0, \quad (29)$$

where $\Psi(\vec{r})$ is the total wave function of the system. The total spin of the system $S = 1$ and the orbital angular momenta $L = 0$ and $L = 2$. Thus the wave function $\Psi(\vec{r})$ should have the following form

$$\Psi(\vec{r}) = \psi_S(\vec{r}) + \psi_D(\vec{r}), \quad (30)$$

where $\psi_S(\vec{r})$ and $\psi_D(\vec{r})$ are the S -wave and D -wave functions, respectively. We use the same matrix method in Ref. [45] to solve this S-D wave couple-channel equation.

We detach the terms related to the kinetic-energy-operator ∇^2 from $V(\vec{r})$ and re-write Eq. (29) as

$$(-\frac{\hbar^2}{2\mu}\nabla^2 - \frac{\hbar^2}{2\mu}[\nabla^2\alpha(r) + \alpha(r)\nabla^2] + \widetilde{V}(\vec{r}) - E)\Psi(\vec{r}) = 0 \quad (31)$$

with

$$\nabla^2 = \frac{1}{r} \frac{d^2}{dr^2} r - \frac{\vec{L}^2}{r^2}, \quad (32)$$

in which $\alpha(r)$ is

$$\begin{aligned} \alpha(r) = & (-2\mu)[-C_\rho \frac{\beta^2 g_v^2}{2m^{*2}}(\vec{\epsilon}_b \cdot \vec{\epsilon}_a^\dagger)(\vec{\epsilon}_{b'} \cdot \vec{\epsilon}_{a'}^\dagger)\mathcal{F}_{4t2\rho} \\ & - C_\rho \frac{\beta^2 g_v^2}{2m^{*2}}(\vec{\epsilon}_b \cdot \vec{\epsilon}_a^\dagger)(\vec{\epsilon}_{b'} \cdot \vec{\epsilon}_{a'}^\dagger)\mathcal{F}_{4t2\omega}] \end{aligned} \quad (33)$$

The total Hamiltonian contains three angular momentum related operators $(\vec{\epsilon}_b \cdot \vec{\epsilon}_a^\dagger)(\vec{\epsilon}_{b'} \cdot \vec{\epsilon}_{a'}^\dagger)$, S'_{12} , $(\vec{\epsilon}_b \times \vec{\epsilon}_a^\dagger)(\vec{\epsilon}_{b'} \times \vec{\epsilon}_{a'}^\dagger)$, \widetilde{S}_{12} , $i(\vec{\epsilon}_{b'} \cdot \vec{\epsilon}_{a'}^\dagger)[(\vec{\epsilon}_a^\dagger \times \vec{\epsilon}_b) \cdot \vec{L}]$, which corresponds to the spin-spin interaction, spin orbit force and tensor force respectively. They act on the S and D-wave coupled wave functions $\phi_S + \phi_D$ and split the total effective potential $\widetilde{V}(\vec{r})$ into the subpotentials $V_{SS}(r)$, $V_{SD}(r)$, $V_{DS}(r)$ and $V_{DD}(r)$. The matrix form reads

$$\begin{aligned} \langle \phi_S + \phi_D | (\vec{\epsilon}_b \cdot \vec{\epsilon}_a^\dagger)(\vec{\epsilon}_{b'} \cdot \vec{\epsilon}_{a'}^\dagger) \widetilde{V}(\vec{r}) | \phi_S + \phi_D \rangle \\ = \begin{pmatrix} V_{SS}(r) & 0 \\ 0 & V_{DD}(r) \end{pmatrix} \end{aligned} \quad (34)$$

$$\langle \phi_S + \phi_D | S'_{12} \widetilde{V}(\vec{r}) | \phi_S + \phi_D \rangle = \begin{pmatrix} 0 & \frac{1}{\sqrt{2}} V_{SD}(r) \\ \frac{1}{\sqrt{2}} V_{DS}(r) & -\frac{1}{2} \end{pmatrix} \quad (35)$$

$$\begin{aligned} \langle \phi_S + \phi_D | (\vec{\epsilon}_b \times \vec{\epsilon}_a^\dagger)(\vec{\epsilon}_{b'} \times \vec{\epsilon}_{a'}^\dagger) \widetilde{V}(\vec{r}) | \phi_S + \phi_D \rangle \\ = \begin{pmatrix} V_{SS}(r) & 0 \\ 0 & V_{DD}(r) \end{pmatrix} \end{aligned} \quad (36)$$

$$\langle \phi_S + \phi_D | \widetilde{S}_{12} \widetilde{V}(\vec{r}) | \phi_S + \phi_D \rangle = \begin{pmatrix} 0 & -\sqrt{2} V_{SD}(r) \\ -\sqrt{2} V_{DS}(r) & 1 \end{pmatrix} \quad (37)$$

$$\begin{aligned} \langle \phi_S + \phi_D | i(\vec{\epsilon}_{b'} \cdot \vec{\epsilon}_{a'}^\dagger)[(\vec{\epsilon}_a^\dagger \times \vec{\epsilon}_b) \cdot \vec{L}] \widetilde{V}(\vec{r}) | \phi_S + \phi_D \rangle \\ = \begin{pmatrix} 0 & 0 \\ 0 & \frac{3}{2} V_{DD}(r) \end{pmatrix} \end{aligned} \quad (38)$$

III. NUMERICAL RESULTS FOR THE $B^*\bar{B}^*$ SYSTEM

We diagonalize the Hamiltonian matrix to obtain the eigenvalue and eigenvector. If there exists a negative eigenvalue, there exists a bound state. The corresponding eigenvector is the wave function. We use the variation principle to solve the equation. We change the variable parameter to get the lowest eigenvalue. We also change the number of the basis functions to reach a stable result.

A. $Z_b(10650)$

Since the mass of the charged bottomonium-like state $Z_b(10650)$ is close to the $B^*\bar{B}^*$ system, we first consider the possibility of the $B^*\bar{B}^*$ molecule with $I^G = 1^+$, $J^{PC} = 1^{+-}$. In order to reflect the recoil correction of the momentum-related terms, we plot the effective potential of the S-wave and D-wave with or without the momentum-related terms in Fig. 2. V_s and V_d are the effective potentials of the S-wave and D-wave interactions after adding the momentum-related terms. V'_s and V'_d are the effective potentials of the S-wave and D-wave interactions without the momentum-related terms. Fig. 2 C corresponds to the $I^G = 1^+$, $J^{PC} = 1^{+-}$ $B^*\bar{B}^*$ system, where the curves of V_s and V'_s , and V_d and V'_d are almost overlapping. In other words, the recoil correction is small.

We collect the numerical results in Table III. E and E' are the eigenenergy of Hamiltonian with and without the momentum-related terms, respectively. The fourth, fifth and sixth column represent the contribution of S -wave, D -wave, and spin-orbit force components, respectively. The last column is the mass of $B^*\bar{B}^*$ as a molecular state of $I^G = 1^+$, $J^{PC} = 1^{+-}$. When the cut off lies within 2.2 – 2.8 GeV, there exists a bound-state. The binding energy with the recoil correction is between 0.97–15.15 MeV. The binding energy without the recoil correction is between 0.94 – 14.98 MeV. When the cutoff parameter $\Lambda = 2.2$ GeV, the binding energy is 0.97 MeV, and the recoil correction is only -0.03 MeV. The contribution from the spin-orbit force is as small as 0.001 MeV. When the cutoff parameter $\Lambda = 2.8$ GeV, the binding energy is 15.15 MeV, and the recoil correction is -0.07 MeV. The correspondence spin-orbit force contribution is 0.02 MeV, which is also small compared with the binding energy. The recoil correction and the contribution of the spin-orbit are very small. However the recoil correction is favorable to the formation of the $B^*\bar{B}^*$ molecular state with $I^G = 1^+$, $J^{PC} = 1^{+-}$.

TABLE III: The bound state solution of the $B^*\bar{B}^*$ system with $I^G = 1^+$, $J^{PC} = 1^{+-}$ (in unit of MeV) and different Λ . E and E' is the eigenenergy of the system with and without the momentum-related terms respectively. We also list the separate contribution to the energy from the S -wave, D -wave and spin-orbit force components respectively in the fourth, fifth and sixth column. The last column is the mass of the $B^*\bar{B}^*$ system with $I^G = 1^+$, $J^{PC} = 1^{+-}$ as a molecular state.

$\Lambda(\text{GeV})$		Eigenvalue				Mass (MeV)
		total	S	D	LS	
2.2	E	-0.97	13.15	0.15	0.001	10649.03
	E'	-0.94	-12.91	-0.15	-	10649.06
2.4	E	-3.49	-28.68	0.32	0.004	10646.51
	E'	-3.43	-28.27	0.32	-	10646.57
2.6	E	-8.04	-49.81	0.56	0.01	10641.96
	E'	-7.94	-49.19	0.55	-	10642.06
2.8	E	-15.15	-77.53	0.88	0.02	10634.85
	E'	-14.98	-76.66	0.87	-	10635.02

From Fig 3 C, it is clear that the π exchange is much more important than the other meson-exchanges. Considering that the coupling constant g is extracted from the D^* decay width with some uncertainty, we multiply g by a factor from 0.99 to 1.1 to check the dependence of the binding energy on this parameter. The numerical results are listed in Table IV. The binding energy with the recoil correction varies from 6.39 – 36.81 MeV. The binding energy without the recoil correction varies from 6.3 – 36.57 MeV. The binding energy is sensitive to the coupling constant.

B. The $B^*\bar{B}^*$ system with $I^G = 1^-$, $J^{PC} = 1^{++}$

For the $B^*\bar{B}^*$ system with $I^G = 1^-$, $J^{PC} = 1^{++}$, there is no bound state when the cutoff varies in a reasonable range. We multiply the coupling constant g by a factor to investigate the

TABLE IV: The $B^*\bar{B}^*$ system with $I^G = 1^+$, $J^{PC} = 1^{+-}$ (in units of MeV) and different coupling constant g and $\Lambda = 2.0$ GeV. The other notations are the same as in Table III.

$\Lambda(\text{GeV})$		Eigenvalue				Mass (MeV)
		Total	S	D	LS	
$g \cdot 0.99$	E	-6.39	-43.28	0.49	0.01	10643.61
	E'	-6.30	-42.70	0.49	-	10643.7
g	E	-8.04	-49.81	0.56	0.01	10641.96
	E'	-7.94	-49.19	0.55	-	10642.06
$g \cdot 1.01$	E	-9.91	-56.68	0.63	0.01	10640.09
	E'	-9.79	-56.02	0.63	-	10640.21
$g \cdot 1.1$	E	-36.81	-132.98	1.32	0.02	10613.19
	E'	-36.57	-131.96	1.31	-	10613.43

dependence of g . We list the results in Table V. The cutoff parameter is fixed at $\Lambda = 2.0$ GeV. There appears a bound state when g increases by a factor 1.3. When the factor changes from 1.3 – 1.5, the binding energy with recoil correction is between 0.82 – 19.25 MeV. The binding energy without the recoil correction is between 0.8 – 19.18 MeV. When the binding energy is 0.82, the recoil correction is -0.02 MeV, and the contribution of the spin-orbit is 0.004 MeV. When the binding energy is 19.25 MeV, the the recoil correction is -0.07 MeV, and the contribution of the spin-orbit force is 0.04 MeV. From Fig 2 D, the effect of the recoil correction is very small for the $B^*\bar{B}^*$ system with $I^G = 1^-$, $J^{PC} = 1^{++}$. But it is favorable for the formation of the molecular state. Fig 3 D shows the contributions of each meson-exchange.

TABLE V: The $B^*\bar{B}^*$ system with $I^G = 1^-$, $J^{PC} = 1^{++}$ (in units of MeV) with the variation of the coupling constant g and $\Lambda = 2.0$ GeV. The other notations are the same as in Table III.

$\Lambda(\text{GeV})$		Eigenvalue				Mass (MeV)
		Total	S	D	LS	
$g \cdot 1.3$	E	-0.82	1.99	-2.23	0.004	10649.18
	E'	-0.80	1.97	-2.21	-	10649.2
$g \cdot 1.4$	E	-6.68	7.73	-8.94	0.02	10643.32
	E'	-6.63	7.69	-8.92	-	10643.37
$g \cdot 1.5$	E	-19.25	15.41	-18.71	0.04	10630.75
	E'	-19.18	15.38	-18.70	-	10630.82

C. The $B^*\bar{B}^*$ system with $I^G = 0^-$, $J^{PC} = 1^{+-}$

We also investigate the $B^*\bar{B}^*$ system with $I^G = 0^-$, $J^{PC} = 1^{+-}$. The effective potential and the meson-exchange contribution are shown in Fig 2 and 3 A. The recoil correction is large. The numerical results are listed in Table VI. The cutoff varies from 1.0 – 1.3 GeV. The binding energy with the recoil correction is around 0 – 41.69 MeV. The binding energy without the recoil correction is between 0.3 – 53.47 MeV. When

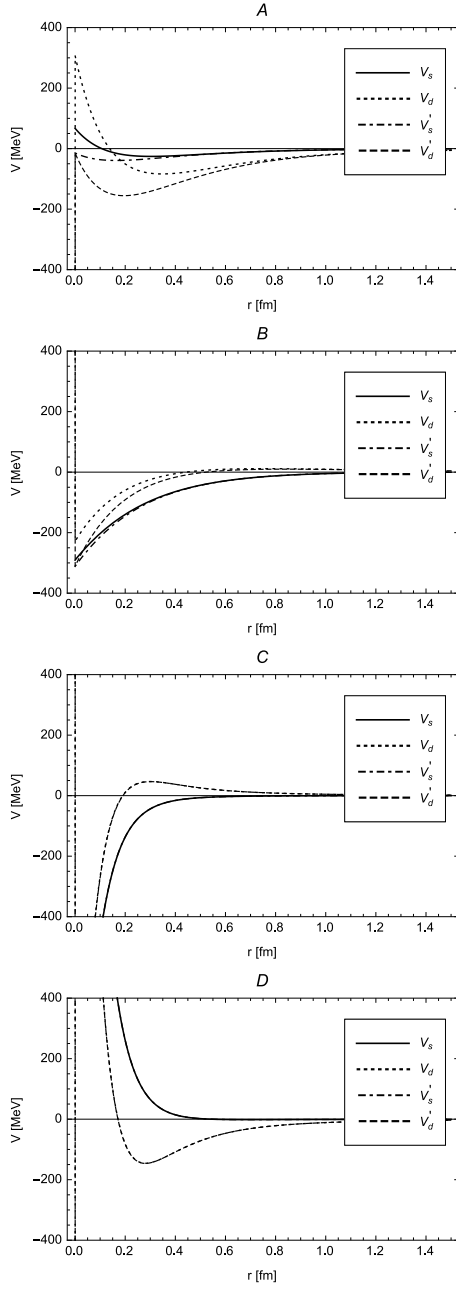


FIG. 2: The effective potential of the $B^* \bar{B}^*$ system. The Labels A,B,C, and D correspond to the four cases $I = 0^-, J^{PC} = 1^{+-}$; $I = 0^+, J^{PC} = 1^{+-}$; $I = 1^+, J^{PC} = 1^{+-}$; and $I = 1^-, J^{PC} = 1^{+-}$, respectively from top to bottom. V_s and V_d are the effective potentials of the S -wave and D -wave interactions with the momentum-related terms, while V'_s and V'_d are the S -wave and D -wave effective potentials without the momentum-related terms.

the cutoff parameter $\Lambda = 1.0$ GeV, there is no bound state after adding the recoil correction. The recoil correction is 0.3 MeV. When the cutoff parameter $\Lambda = 1.3$ GeV, the binding energy is 41.69 MeV. The recoil correction is 12.05 MeV, and the contribution of the spin-orbit force is 4.3 MeV. In this case, the recoil correction is significant and it is almost as big as the

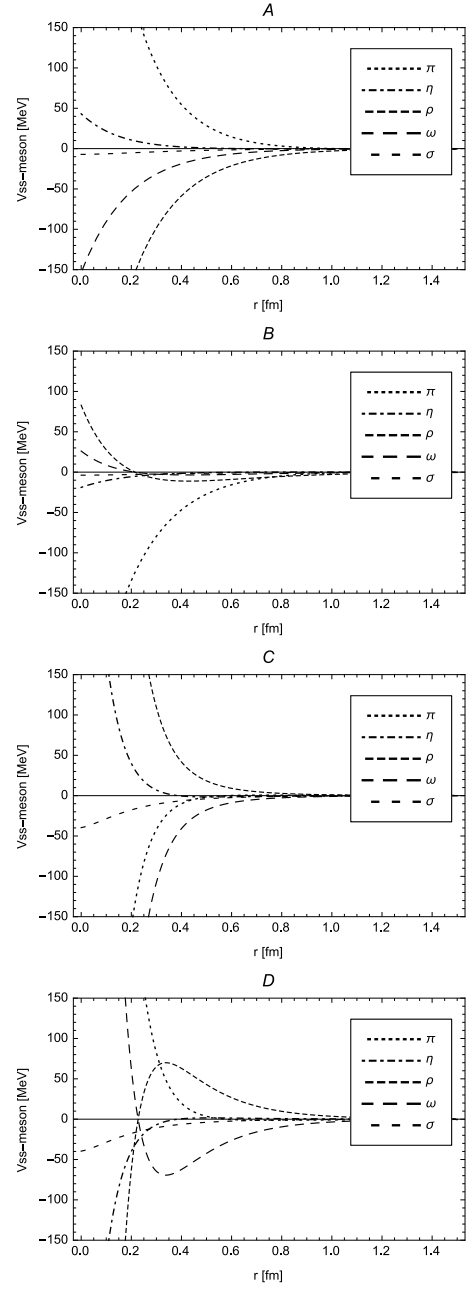


FIG. 3: The effective potential from the different meson exchange in the $B^* \bar{B}^*$ system. Labels A,B,C,D are the same as in Fig. 2.

D -wave contribution. But it is unfavorable for the formation of the molecule.

D. The $B^* \bar{B}^*$ system with $I^G = 0^+, J^{PC} = 1^{++}$

For the $B^* \bar{B}^*$ system with $I^G = 0^+, J^{PC} = 1^{++}$, V_s and V'_s are clearly different within the range of $0 - 0.6$ fm as can be seen from Fig 2 B. Fig 3 B shows the contributions of each meson-exchange. The recoil correction in this system is im-

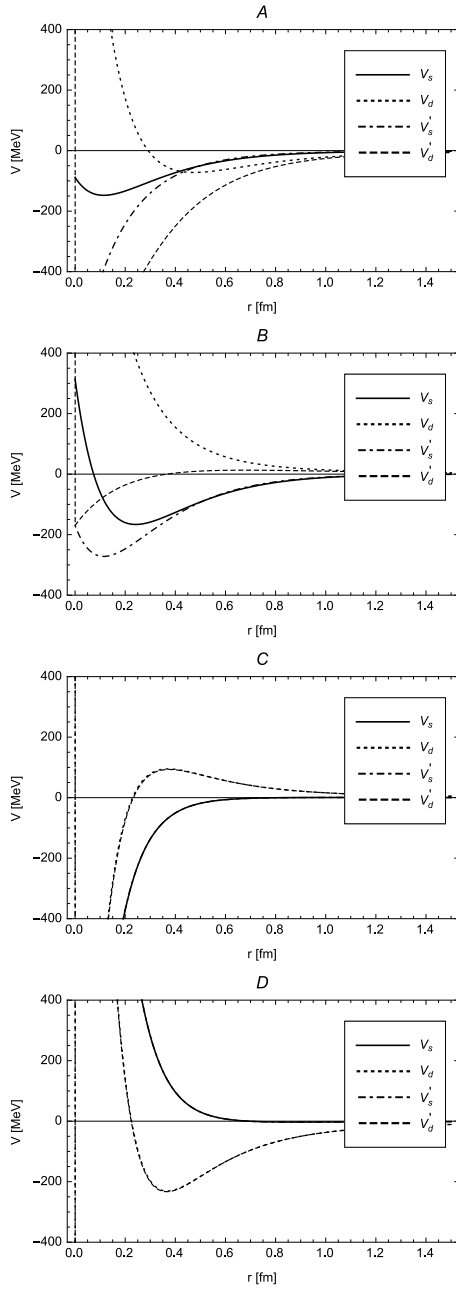


FIG. 4: The effective potential of the $D^* \bar{D}^*$ system. The Labels A,B,C, and D correspond to the four cases $I = 0^-, J^{PC} = 1^{+-}$; $I = 0^+, J^{PC} = 1^{+-}$; $I = 1^+, J^{PC} = 1^{+-}$; and $I = 1^-, J^{PC} = 1^{+-}$, respectively from top to bottom. V_s and V_d are the effective potentials of the S -wave and D -wave interactions with the momentum-related terms, while V'_s and V'_d are the S -wave and D -wave effective potentials without the momentum-related terms.

portant. The results are listed in Table VII. When the variation of the cutoff parameter is between 0.9 – 1.2 GeV, the binding energy with the recoil correction changes from 6.71 to 59.74 MeV. The binding energy without the recoil correction changes from 6.86 – 63.76 MeV. When the cutoff parameter $\Lambda = 0.9$ GeV, the binding energy is 6.71 MeV. The re-

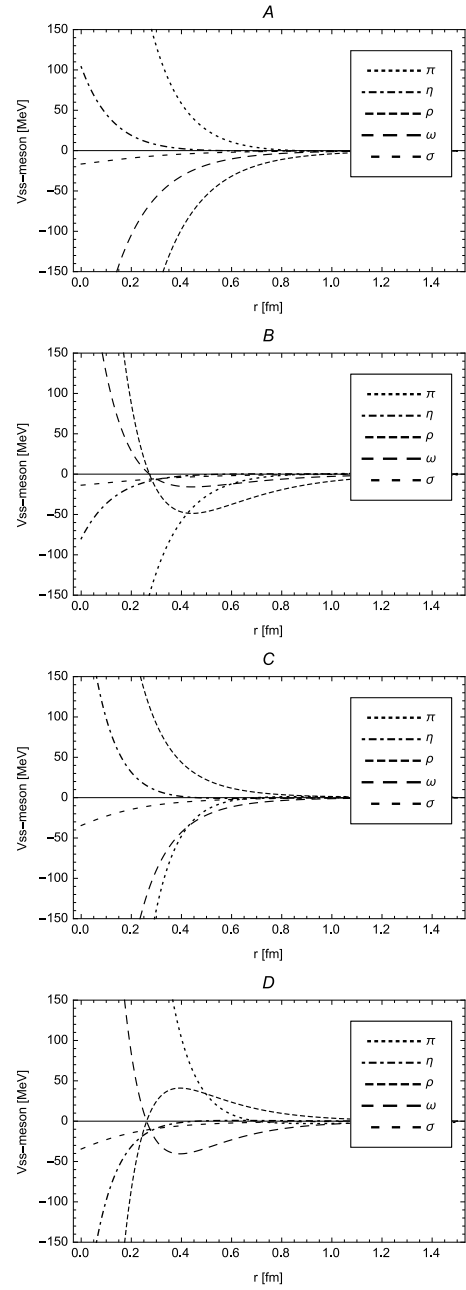


FIG. 5: The effective potential from the different meson exchange in the $D^* \bar{D}^*$ system. Labels A,B,C,D are the same as in Fig. 4.

coil correction is 0.15 MeV, and the contribution of the spin-orbit force is 0.03 MeV. When the cutoff parameter $\Lambda = 1.2$ GeV, the binding energy is 63.76 MeV. The recoil correction is 4.02 MeV, and the contribution of the spin-orbit force is 1.39 MeV. The recoil correction is of the same order as the D -wave contribution. Moreover, it increase with the binding energy. Therefore, the recoil effect can not be neglected. However, the recoil correction is unfavorable for the formation of the molecule in this system.

TABLE VI: The bound state solutions of the $B^*\bar{B}^*$ system with $I^G = 0^-, J^{PC} = 1^{+-}$ (in unit of MeV) with the cutoff Λ . The other notations are the same as in Table III.

$\Lambda(\text{GeV})$	Eigenvalue					Mass (MeV)
	total	S	D	LS		
1.0	E	-	-	-	-	10650
	E'	-0.30	-0.59	-0.07	-	10649.7
1.1	E	-4.34	-1.88	-3.08	0.42	10645.66
	E'	-5.51	-2.19	-4.29	-	10644.49
1.2	E	-17.07	-9.05	-7.92	1.68	10632.93
	E'	-21.79	-12.09	-11.12	-	10628.21
1.3	E	-41.69	-24.61	-14.80	4.30	10608.31
	E'	-53.74	-30.81	-24.77	-	10596.26

TABLE VII: The bound state solutions of the $B^*\bar{B}^*$ system with $I^G = 0^-, J^{PC} = 1^{+-}$ (in unit of MeV) with the cutoff Λ . The other notations are the same as in Table III.

$\Lambda(\text{GeV})$	Eigenvalue					Mass (MeV)
	total	S	D	LS		
0.9	E	-6.71	-22.27	0.18	0.03	10643.29
	E'	-6.86	-22.85	0.15	-	10643.14
1.0	E	-19.36	-43.77	0.25	0.18	10630.64
	E'	-20.15	-46.10	0.03	-	10629.85
1.1	E	-37.51	-65.91	0.53	0.58	10612.49
	E'	-39.58	-71.13	-0.2	-	10610.42
1.2	E	-59.74	-86.12	1.34	1.39	10590.26
	E'	-63.76	-94.99	-0.43	-	10586.24

IV. NUMERICAL RESULTS FOR $D^*\bar{D}^*$ SYSTEM

A. $D^*\bar{D}^*$ system with $I^G = 1^+, J^{PC} = 1^{+-}$

Due to the isospin symmetry, the interaction in the $D^*\bar{D}^*$ system has the same form with the $B^*\bar{B}^*$ system. Therefore, we repeat the same investigations for the $D^*\bar{D}^*$ system. $Z_c(4025)$ was observed in the π^\mp recoil mass spectrum in the process $e^-e^+ \rightarrow (D^*\bar{D}^*)^\pm\pi^\mp$ [14]. The mass of $Z_c(4025)$ is close to the threshold of $D^*\bar{D}^*$, and $Z_c(4025)$ has the quantum with $I^G = 1^+, J^{PC} = 1^{+-}$. Therefore we first consider the possibility of the $D^*\bar{D}^*$ system as the molecular state with the quantum number $I^G = 1^+, J^{PC} = 1^{+-}$.

From Fig 4 C, the curves of V_s and V'_s are almost overlapping, same as those of V_d and V'_d , which indicates that the recoil correction is small. Fig 5 C shows that π meson-exchange plays an important role in the interaction.

Unfortunately, we did not get a bound state within a reasonable range of the cutoff parameter and coupling constant. The value of the pionic coupling constant was extracted from the decay width of the D^* meson where the pion is on the mass-shell. However we need the value of the coupling constant in the potential where the pion is off-shell. Considering the big

influence of the π meson-exchange, we multiply the coupling constant g by a factor to check the dependence of the results on g . The cutoff parameter is fixed at $\Lambda = 2.0$ GeV. The results are shown in Table VIII.

When the factor reaches 1.6, there appears the bound state. The binding energy with the recoil correction is 1.15 MeV and the recoil correction is -0.05 MeV. The contribution of the spin-orbit force is 0.01 MeV. When the factor is 1.8, the binding energy with recoil correction is 28.62 MeV, and the recoil correction is -0.28 MeV. The contribution of the spin-orbit force is 0.07 MeV. As in the $B^*\bar{B}^*$ system with $I^G = 1^+, J^{PC} = 1^{+-}$, the recoil correction is not so big. But the recoil correction is favorable for the formation of $D^*\bar{D}^*$ molecular state. In other words, the existence of the $D^*\bar{D}^*$ molecule depends on the coupling constant g sensitively.

TABLE VIII: The $D^*\bar{D}^*$ system with $I^G = 1^+, J^{PC} = 1^{+-}$ (in units of MeV) with the variation of coupling constant g and $\Lambda = 2.0$ GeV. The other notations are the same as in Table III.

$\Lambda(\text{GeV})$	Eigenvalue					Mass (MeV)
	Total	S	D	LS		
$g \cdot 1.6$	E	-1.15	-22.96	0.37	0.01	4019.35
	E'	-1.10	-22.27	0.36	-	4019.40
$g \cdot 1.7$	E	-10.19	-75.21	1.10	0.04	4010.31
	E'	-10.03	-74.02	1.08	-	4010.47
$g \cdot 1.8$	E	-28.62	-139.80	1.80	0.07	3991.88
	E'	-28.34	-138.16	1.77	-	3992.16

B. $D^*\bar{D}^*$ system with $I^G = 1^-, J^{PC} = 1^{++}$

We also investigate the $D^*\bar{D}^*$ system with $I^G = 1^-, J^{PC} = 1^{++}$. From Fig 4 D and Fig 5 D, the recoil correction is very small while the π meson-exchange plays an significant role in the interaction. There also does not exist a bound state when the cutoff parameter is within a reasonable range. We also study the variation with the coupling constant g . The results are shown in Table IX.

The recoil correction is also very small in this system. For example, when the binding energy is 4.71 MeV, the recoil correction is only -0.03 MeV, and the contribution of the spin-orbit force is 0.05 MeV. And the recoil correction is favorable for the formation of the molecular state.

C. The $D^*\bar{D}^*$ system with $I^G = 0^-, J^{PC} = 1^{+-}$ and $I^G = 0^+, J^{PC} = 1^{++}$

For the isoscalar $D^*\bar{D}^*$ system, V_s and V'_s are very different from Fig. 4 A and B. Fig 5 A and B show the contributions of each meson-exchange. The recoil contribution is large and unfavorable for the formation of the molecular states. There exist bound states for the isoscalar $D^*\bar{D}^*$ system with different C-parity. The results are listed in Tables X and XI.

TABLE IX: The $D^*\bar{D}^*$ system with $I^G = 1^-, J^{PC} = 1^{++}$ (in units of MeV) with the variation of coupling constant g and $\Lambda = 2.0$ GeV. The other notations are the same as in Table III.

$\Lambda(\text{GeV})$		Eigenvalue				Mass (MeV)
		Total	S	D	LS	
$g \cdot 2.4$	E	-4.71	7.72	-8.47	0.05	4015.79
	E'	-4.68	7.69	-8.49	-	4015.82
$g \cdot 2.5$	E	-11.05	13.22	-14.96	0.09	4009.45
	E'	-11.02	13.19	-15.02	-	4009.48
$g \cdot 2.6$	E	-20.37	19.46	-22.76	0.13	4000.13
	E'	-20.34	19.43	-22.86	-	4000.16

For the $J^{PC} = 1^{+-}$ case, when cutoff parameter changes from 1.4 – 1.6 GeV, the binding energy with the recoil correction is within 0.58 – 17.09 MeV. The binding energy without the recoil correction is within 3.83 – 17.09 MeV. The recoil correction is large. For example, when the binding energy is 0.58 MeV, the recoil correction is 3.25 MeV, even bigger than the binding energy itself. The contribution of the spin-orbit force is 0.4 MeV, which is almost as large as the binding energy.

For the $J^{PC} = 1^{++}$ case, when cutoff parameter changes from 1.3 – 1.6 GeV, the binding energy with the recoil correction is within 9.13 – 43.25 MeV. The binding energy without the recoil correction is within 10.59 – 49.23 MeV. The recoil correction is also significant. For example, when the binding energy is 9.13 MeV, the recoil correction is 1.46 MeV. The contribution of the spin-orbit force is 0.75 MeV, which is almost as large as D-wave contribution. When the binding energy is 43.25 MeV, the recoil correction is 5.98 MeV. The contribution of the spin-orbit force is 5.21 MeV.

TABLE X: The $D^*\bar{D}^*$ system with $I^G = 0^-, J^{PC} = 1^{+-}$ (in unit of MeV). The other notations are the same as in Table III.

$\Lambda(\text{GeV})$		Eigenvalue				Mass (MeV)
		total	S	D	LS	
1.4	E	-0.58	-5.03	-0.43	0.40	4019.92
	E'	-3.83	-15.14	-3.06	-	4016.67
1.5	E	-5.67	-19.23	-1.45	1.91	4014.83
	E'	-17.25	-44.41	-8.84	-	4003.25
1.6	E	-17.09	-40.12	-2.52	4.76	4003.41
	E'	-42.61	-79.61	-17.73	-	3977.89

V. SUMMARY AND DISCUSSION

With the one-boson-exchange model, we have systematically studied the possible loosely bound $B^*\bar{B}^*$ and $D^*\bar{D}^*$ systems with (1) $I^G = 0^+, J^{PC} = 1^{++}$, (2) $I^G = 0^-, J^{PC} = 1^{+-}$, (3) $I^G = 1^+, J^{PC} = 1^{+-}$ and (4) $I^G = 1^-, J^{PC} = 1^{++}$. We consider the π, η, σ, ρ and ω meson exchange in the derivation

TABLE XI: The $D^*\bar{D}^*$ system with $I^G = 0^+, J^{PC} = 1^{++}$ (in unit of MeV). The other notations are the same as in Table III.

$\Lambda(\text{GeV})$		Eigenvalue				Mass (MeV)
		total	S	D	LS	
1.3	E	-9.13	-34.43	1.04	0.75	4011.37
	E'	-10.59	-42.22	-0.15	-	4009.91
1.4	E	-18.20	-49.42	2.25	1.66	4002.3
	E'	-20.87	-61.74	-0.29	-	3999.63
1.5	E	-29.64	-63.30	4.22	3.11	3990.86
	E'	-33.82	-80.59	0.57	-	3986.68
1.6	E	-43.25	-76.05	7.17	5.21	3977.25
	E'	-49.23	-98.50	1.10	-	3971.27

of the potential. We keep the momentum dependent terms in the polarization vector of the two heavy mesons and introduce the momentum-related terms in the interaction, which lead to the recoil correction and spin-orbit force at $O(1/M^2)$.

The $B^*\bar{B}^*$ system with $I^G = 1^+, J^{PC} = 1^{+-}$ can form the molecular state, which may correspond to the heavier Z_b state observed by Belle collaboration. When the cutoff parameter is within 2.2 – 2.6 GeV, the binding energy is between 0.97 – 15.15 MeV. The recoil correction is small. The contribution of the spin-orbit force is also very small. For example, when the binding energy is 15.15 MeV, the recoil correction is -0.17 MeV. The contribution of the spin-orbit force is 0.02 MeV. But the recoil correction is favorable to the formation of the molecular state. On the other hand, our results shows that the binding energy is sensitive to the pionic coupling constant.

For the isoscalar $B^*\bar{B}^*$ system, there exist a bound state when changing the cutoff parameter. For the $J^{PC} = 1^{+-}$ state, when cutoff parameter is within 1.0 – 1.3 GeV, the binding energy is between 0 – 41.69 MeV. For the $J^{PC} = 1^{++}$ state, when cutoff parameter is within 0.9 – 1.2 GeV, the binding energy is between 6.71 – 59.74 MeV. The recoil correction of the two systems are both large and important. However, they are unfavorable to the formation of the molecular states.

For the $D^*\bar{D}^*$ system with $I^G = 1^+, J^{PC} = 1^{+-}$, we are unable to obtain the bound state within a reasonable cutoff range and the pionic coupling constant g extracted from the D^* decay width. If we enlarge the pionic coupling constant by a factor of 1.6 – 1.8, there appears the bound state with the binding energy around 1.15 – 28.62 MeV. The recoil correction is small. For example, when the binding energy is 28.62 MeV, the recoil correction is -0.28 MeV. The contribution of the spin-orbit force is 0.07 MeV. The recoil correction is favorable for the formation of the molecular state.

For the isoscalar $D^*\bar{D}^*$ system, there exist bound states when changing the cutoff parameter. For the $J^{PC} = 1^{+-}$ state, when the cutoff parameter is within 1.4 – 1.6 GeV, the binding energy is around 0.58 – 42.61 MeV. For the $J^{PC} = 1^{++}$ state, when the cutoff parameter is within 1.3 – 1.6 GeV, the binding energy is around 9.13 – 43.25 MeV. The recoil correction is significant but unfavorable to the formation of the molecular states.

VI. APPENDIX

We collect the lengthy formulae in the appendix.

$$Y(\tilde{m}_\alpha r) = \frac{\exp(\tilde{m}_\alpha r)}{\tilde{m}_\alpha r} \quad (39)$$

$$Z(\tilde{m}_\alpha r) = (1 + \frac{3}{\tilde{m}_\alpha r} + \frac{3}{(\tilde{m}_\alpha r)^2})Y(\tilde{m}_\alpha r) \quad (40)$$

$$Z_1(\tilde{m}_\alpha r) = (\frac{1}{\tilde{m}_\alpha r} + \frac{1}{(\tilde{m}_\alpha r)^2})Y(\tilde{m}_\alpha r) \quad (41)$$

$$Z'(\tilde{m}_\alpha r) = \frac{\sin(\tilde{m}_\alpha r)}{\tilde{m}_\alpha r} - \frac{3}{\tilde{m}_\alpha r} \frac{\sin(\tilde{m}_\alpha r)}{\tilde{m}_\alpha r} + \frac{1}{(\tilde{m}_\alpha r)^2} \frac{\cos(\tilde{m}_\alpha r)}{\tilde{m}_\alpha r}. \quad (42)$$

$$Z'_1(\tilde{m}_\alpha r) = \frac{1}{\tilde{m}_\alpha r} \frac{\sin(\tilde{m}_\alpha r)}{\tilde{m}_\alpha r} + \frac{1}{(\tilde{m}_\alpha r)^2} \frac{\cos(\tilde{m}_\alpha r)}{\tilde{m}_\alpha r} \quad (43)$$

where for system $D\bar{D}^*$

$$\tilde{m}_\pi^2 = (m_D^* - m_D)^2 - m_\pi^2, \quad (44)$$

$$\tilde{m}_{\sigma,\rho,\omega,\eta}^2 = m_{\sigma,\rho,\omega,\eta}^2 - (m_D^* - m_D)^2. \quad (45)$$

for system $B\bar{B}^*$

$$\tilde{m}_{\pi,\sigma,\rho,\omega,\eta}^2 = m_{\pi,\sigma,\rho,\omega,\eta}^2 - (m_B^* - m_B)^2. \quad (46)$$

$$\begin{aligned} \mathcal{F}_{1t\alpha} &= \mathcal{F}\{(\frac{\Lambda^2 - m_\alpha^2}{\Lambda^2 + \vec{q}^2}) \frac{1}{\vec{q}^2 + m_\alpha^2}\} \\ &= m_\alpha Y(m_\alpha r) - \Lambda Y(\Lambda r) - (\Lambda^2 - m_\alpha^2) \frac{e^{-\Lambda r}}{2\Lambda} \end{aligned} \quad (47)$$

$$\begin{aligned} \mathcal{F}_{1u\alpha} &= \mathcal{F}\{(\frac{\Lambda^2 - m_\alpha^2}{\Lambda^2 + \vec{q}^2}) \frac{1}{\vec{q}^2 + \tilde{m}_\alpha^2}\} \\ &= \tilde{m}_\alpha Y(\tilde{m}_\alpha r) - \tilde{\Lambda} Y(\tilde{\Lambda} r) - (\Lambda^2 - m_\alpha^2) \frac{e^{-\tilde{\Lambda} r}}{2\tilde{\Lambda}} \end{aligned} \quad (48)$$

$$\begin{aligned} \mathcal{F}_{2t\alpha} &= \mathcal{F}\{(\frac{\Lambda^2 - m_\alpha^2}{\Lambda^2 + \vec{q}^2}) \frac{\vec{q}^2}{\vec{q}^2 + m_\alpha^2}\} \\ &= m_\alpha^2 [\Lambda Y(\Lambda r) - m_\alpha Y(m_\alpha r)] \\ &\quad + (\Lambda^2 - m_\alpha^2) \Lambda \frac{e^{-\Lambda r}}{2} \end{aligned} \quad (49)$$

$$\begin{aligned} \mathcal{F}_{2u\alpha} &= \mathcal{F}\{(\frac{\Lambda^2 - m_\alpha^2}{\tilde{\Lambda}^2 + \vec{q}^2}) \frac{\vec{q}^2}{\vec{q}^2 + \tilde{m}_\alpha^2}\} \\ &= \tilde{m}_\alpha^2 [\tilde{\Lambda} Y(\tilde{\Lambda} r) - \tilde{m}_\alpha Y(\tilde{m}_\alpha r)] \\ &\quad + (\Lambda^2 - m_\alpha^2) \tilde{\Lambda} \frac{e^{-\tilde{\Lambda} r}}{2} \end{aligned} \quad (50)$$

$$\begin{aligned} \mathcal{F}_{3t\alpha} &= \mathcal{F}\{(\frac{\Lambda^2 - m_\alpha^2}{\Lambda^2 + \vec{q}^2}) \frac{(\vec{\sigma}_1 \cdot \vec{q})(\vec{\sigma}_2 \cdot \vec{q})}{\vec{p}^2 + m_\alpha^2}\} \\ &= \frac{1}{3} \vec{\sigma}_1 \cdot \vec{\sigma}_2 [m_\alpha^2 \Lambda Y(\Lambda r) - m_\alpha^3 Y(m_\alpha r) \\ &\quad + (\Lambda^2 - m_\alpha^2) \Lambda \frac{e^{-\Lambda r}}{2}] \\ &\quad + \frac{1}{3} S_{12} [-m_\alpha^3 Z(m_\alpha r) + \Lambda^3 Z(\Lambda r) \\ &\quad + (\Lambda^2 - m_\alpha^2)(1 + \Lambda r) \frac{\Lambda}{2} Y(\Lambda r)] \\ &= (\vec{\sigma}_1 \cdot \vec{\sigma}_2) \mathcal{F}_{3t1} + S_{12} \mathcal{F}_{3t2} \end{aligned} \quad (51)$$

$$\begin{aligned} \mathcal{F}_{3u\alpha} &= \mathcal{F}\{(\frac{\Lambda^2 - m_\alpha^2}{\tilde{\Lambda}^2 + \vec{q}^2}) \frac{(\vec{\sigma}_1 \cdot \vec{q})(\vec{\sigma}_2 \cdot \vec{q})}{\vec{q}^2 + \tilde{m}_\alpha^2}\} \\ &= \frac{1}{3} \vec{\sigma}_1 \cdot \vec{\sigma}_2 [\tilde{m}_\alpha^2 \tilde{\Lambda} Y(\tilde{\Lambda} r) - \tilde{m}_\alpha^3 Y(\tilde{m}_\alpha r) \\ &\quad + (\Lambda^2 - m_\alpha^2) \tilde{\Lambda} \frac{e^{-\tilde{\Lambda} r}}{2}] \\ &\quad + \frac{1}{3} S_{12} [-\tilde{m}_\alpha^3 Z(\tilde{m}_\alpha r) + \tilde{\Lambda}^3 Z(\tilde{\Lambda} r) \\ &\quad + (\Lambda^2 - m_\alpha^2)(1 + \tilde{\Lambda} r) \frac{\tilde{\Lambda}}{2} Y(\tilde{\Lambda} r)] \\ &= (\vec{\sigma}_1 \cdot \vec{\sigma}_2) \mathcal{F}_{3u1\alpha} + S_{12} \mathcal{F}_{3u2\alpha} \end{aligned} \quad (52)$$

$$\begin{aligned} \mathcal{F}'_{3u\alpha} &= \mathcal{F}\{(\frac{\Lambda^2 - m_\alpha^2}{\tilde{\Lambda}^2 + \vec{q}^2}) \frac{(\vec{\sigma}_1 \cdot \vec{q})(\vec{\sigma}_2 \cdot \vec{q})}{\vec{p}^2 - \tilde{m}_\alpha^2}\} \\ &= \frac{1}{3} \vec{\sigma}_1 \cdot \vec{\sigma}_2 [-\tilde{m}_\alpha^2 \tilde{\Lambda} Y(\tilde{\Lambda} r) - \tilde{m}_\alpha^3 \frac{\cos(\tilde{m}_\alpha r)}{\tilde{m}_\alpha r} \\ &\quad + (\Lambda^2 - m_\alpha^2) \tilde{\Lambda} \frac{e^{-\tilde{\Lambda} r}}{2}] \\ &\quad + \frac{1}{3} S_{12} [\tilde{m}_\alpha^3 Z'(\tilde{m}_\alpha r) + \tilde{\Lambda}^3 Z(\tilde{\Lambda} r) \\ &\quad + (\Lambda^2 - m_\alpha^2)(1 + \tilde{\Lambda} r) \frac{\tilde{\Lambda}}{2} Y(\tilde{\Lambda} r)] \\ &= (\vec{\sigma}_1 \cdot \vec{\sigma}_2) \mathcal{F}'_{3u1\alpha} + S_{12} \mathcal{F}'_{3u2\alpha} \end{aligned} \quad (53)$$

$$\begin{aligned} \mathcal{F}_{4t\alpha} &= \mathcal{F}\{(\frac{\Lambda^2 - m_\alpha^2}{\Lambda^2 + \vec{q}^2}) \frac{\vec{k}^2}{\vec{q}^2 + m_\alpha^2}\} \\ &= \frac{m_\alpha^3}{4} Y(m_\alpha r) - \frac{\Lambda^3}{4} Y(\Lambda r) \\ &\quad - \frac{\Lambda^2 - m_\alpha^2}{4} (\frac{\Lambda r}{2} - 1) \frac{e^{-\Lambda r}}{r} \\ &\quad - \frac{1}{2} \{\nabla^2, m_\alpha Y(m_\alpha r) - \Lambda Y(\Lambda r) - \frac{\Lambda^2 - m_\alpha^2}{2} \frac{e^{-\Lambda r}}{\Lambda}\} \\ &= \mathcal{F}_{4t1\alpha} + \{-\frac{1}{2} \nabla^2, \mathcal{F}_{4t2\alpha}\} \end{aligned} \quad (54)$$

$$\begin{aligned}
\mathcal{F}_{4u\alpha} &= \mathcal{F}\left\{\left(\frac{\Lambda^2 - \tilde{m}_\alpha^2}{\tilde{\Lambda}^2 + \vec{q}^2}\right) \frac{\vec{k}^2}{\vec{q}^2 + \tilde{m}_\alpha^2}\right\} \\
&= \frac{\tilde{m}_\alpha^3}{4} Y(\tilde{m}_\alpha r) - \frac{\tilde{\Lambda}^3}{4} Y(\tilde{\Lambda} r) \\
&\quad - \frac{\Lambda^2 - m_\alpha^2}{4} \left(\frac{\tilde{\Lambda} r}{2} - 1\right) \frac{e^{-\tilde{\Lambda} r}}{r} \\
&\quad - \frac{1}{2} [\nabla^2, \tilde{m}_\alpha Y(\tilde{m}_\alpha r) - \tilde{\Lambda} Y(\tilde{\Lambda} r) - \frac{\Lambda^2 - m_\alpha^2}{2} \frac{e^{-\tilde{\Lambda} r}}{\tilde{\Lambda}}] \\
&= \mathcal{F}_{4u1\alpha} + \left\{-\frac{1}{2} \nabla^2, \mathcal{F}_{4u2\alpha}\right\} \quad (55)
\end{aligned}$$

$$\begin{aligned}
\mathcal{F}_{5t\alpha} &= \mathcal{F}\left\{i\left(\frac{\Lambda^2 - m_\alpha^2}{\Lambda^2 + \vec{q}^2}\right) \frac{\vec{S} \cdot (\vec{q} \times \vec{k})}{\vec{q}^2 + m_\alpha^2}\right\} \\
&= \vec{S} \cdot \vec{L} [-m_\alpha^3 Z_1(m_\alpha r) + \Lambda^3 Z_1(\Lambda r) \\
&\quad + (\Lambda^2 - m_\alpha^2) \frac{e^{-\Lambda r}}{2r}] \\
&= \vec{S} \cdot \vec{L} \mathcal{F}_{5t0\alpha} \quad (56)
\end{aligned}$$

$$\begin{aligned}
\mathcal{F}_{5u\alpha} &= \mathcal{F}\left\{i\left(\frac{\Lambda^2 - m_\alpha^2}{\tilde{\Lambda}^2 + \vec{q}^2}\right) \frac{\vec{S} \cdot (\vec{q} \times \vec{k})}{\vec{q}^2 + \tilde{m}_\alpha^2}\right\} \\
&= \vec{S} \cdot \vec{L} [-\tilde{m}_\alpha^3 Z_1(\tilde{m}_\alpha r) + \tilde{\Lambda}^3 Z_1(\tilde{\Lambda} r) \\
&\quad + (\Lambda^2 - m_\alpha^2) \frac{e^{-\tilde{\Lambda} r}}{2r}] \\
&= \vec{S} \cdot \vec{L} \mathcal{F}_{5u0\alpha} \quad (57)
\end{aligned}$$

$$\begin{aligned}
\mathcal{F}'_{5u\alpha} &= \mathcal{F}\left\{i\left(\frac{\Lambda^2 - m_\alpha^2}{\tilde{\Lambda}^2 + \vec{q}^2}\right) \frac{\vec{S} \cdot (\vec{q} \times \vec{k})}{\vec{q}^2 + \tilde{m}_\alpha^2}\right\} \\
&= \vec{S} \cdot \vec{L} [-\tilde{m}_\alpha^3 Z'_1(\tilde{m}_\alpha r) + \tilde{\Lambda}^3 Z_1(\tilde{\Lambda} r) \\
&\quad + (\Lambda^2 - m_\alpha^2) \frac{e^{-\tilde{\Lambda} r}}{2r}] \\
&= \vec{S} \cdot \vec{L} \mathcal{F}'_{5u0\alpha} \quad (58)
\end{aligned}$$

$$\begin{aligned}
\mathcal{F}_{6u\alpha} &= \mathcal{F}\left\{\left(\frac{\Lambda^2 - m_\alpha^2}{\tilde{\Lambda}^2 + \vec{q}^2}\right) \frac{(\vec{\sigma}_1 \cdot \vec{k})(\vec{\sigma}_2 \cdot \vec{k})}{\vec{p}^2 + \tilde{m}_\alpha^2}\right\} \\
&= -\frac{\vec{\sigma}_1 \cdot \vec{\sigma}_2}{4} [\tilde{m}_\alpha^3 Y(\tilde{m}_\alpha r) - (\tilde{\Lambda})^3 Y(\tilde{\Lambda} r) \\
&\quad - (\Lambda^2 - m_\alpha^2) \tilde{\Lambda} \frac{e^{-\tilde{\Lambda} r}}{2}] \\
&\quad + \frac{1}{3} (S_{12} + \vec{\sigma}_1 \cdot \vec{\sigma}_2) \left[\left(1 + \frac{3}{\tilde{m}_\alpha r}\right) \tilde{m}_\alpha^2 Y(\tilde{\Lambda} r) \right. \\
&\quad \left. - \left(1 + \frac{3}{\tilde{\Lambda} r}\right) (\tilde{\Lambda})^2 Y(\tilde{\Lambda} r) \right. \\
&\quad \left. - (\Lambda^2 - m_\alpha^2) \left(\tilde{\Lambda} + \frac{2}{r}\right) \frac{e^{-\tilde{\Lambda} r}}{2\tilde{\Lambda}} \right] \nabla \\
&\quad - \frac{1}{3} (S_{12} + \vec{\sigma}_1 \cdot \vec{\sigma}_2) [\tilde{m}_\alpha Y(\tilde{m}_\alpha r) - \tilde{\Lambda} Y(\tilde{\Lambda} r) \\
&\quad - (\Lambda^2 - m_\alpha^2) \frac{e^{-\tilde{\Lambda} r}}{2\tilde{\Lambda}}] \nabla^2 \\
&= -\frac{\vec{\sigma}_1 \cdot \vec{\sigma}_2}{4} \mathcal{F}_{6u1\alpha} + \frac{1}{3} (S_{12} + \vec{\sigma}_1 \cdot \vec{\sigma}_2) \mathcal{F}_{6u2\alpha} \\
&\quad - \frac{1}{3} (S_{12} + \vec{\sigma}_1 \cdot \vec{\sigma}_2) \mathcal{F}_{6u3\alpha} \quad (59)
\end{aligned}$$

$$\begin{aligned}
\mathcal{F}'_{6u\alpha} &= \mathcal{F}\left\{\left(\frac{\Lambda^2 - m_\alpha^2}{\tilde{\Lambda}^2 + \vec{q}^2}\right) \frac{(\vec{\sigma}_1 \cdot \vec{k})(\vec{\sigma}_2 \cdot \vec{k})}{\vec{p}^2 + \tilde{m}_\alpha^2}\right\} \\
&= -\frac{\vec{\sigma}_1 \cdot \vec{\sigma}_2}{4} [\tilde{m}_\alpha^3 \frac{\cos(M_\alpha r)}{\tilde{m}_\alpha r} - (\tilde{\Lambda})^3 Y(\tilde{\Lambda} r) \\
&\quad - (\Lambda^2 - m_\alpha^2) \tilde{\Lambda} \frac{e^{-\tilde{\Lambda} r}}{2}] \\
&\quad + \frac{1}{3} (S_{12} + \vec{\sigma}_1 \cdot \vec{\sigma}_2) \left[\left(\frac{\sin(\tilde{m}_\alpha r)}{\tilde{m}_\alpha r} + \frac{3}{\tilde{m}_\alpha r} \frac{\cos(\tilde{m}_\alpha r)}{\tilde{m}_\alpha r}\right) \tilde{m}_\alpha^2 \right. \\
&\quad \left. - \left(1 + \frac{3}{\tilde{\Lambda} r}\right) (\tilde{\Lambda})^2 Y(\tilde{\Lambda} r) - (\Lambda^2 - m_\alpha^2) \left(\tilde{\Lambda} + \frac{2}{r}\right) \frac{e^{-\tilde{\Lambda} r}}{2\tilde{\Lambda}} \right] \nabla \\
&\quad - \frac{1}{3} (S_{12} + \vec{\sigma}_1 \cdot \vec{\sigma}_2) [\tilde{m}_\alpha \frac{\cos(\tilde{m}_\alpha r)}{\tilde{m}_\alpha r} - \tilde{\Lambda} Y(\tilde{\Lambda} r) \\
&\quad - (\Lambda^2 - m_\alpha^2) \frac{e^{-\tilde{\Lambda} r}}{2\tilde{\Lambda}}] \nabla^2 \\
&= -\frac{\vec{\sigma}_1 \cdot \vec{\sigma}_2}{4} \mathcal{F}'_{6u1\alpha} + \frac{1}{3} (S_{12} + \vec{\sigma}_1 \cdot \vec{\sigma}_2) \mathcal{F}'_{6u2\alpha} \\
&\quad - \frac{1}{3} (S_{12} + \vec{\sigma}_1 \cdot \vec{\sigma}_2) \mathcal{F}'_{6u3\alpha} \quad (60)
\end{aligned}$$

ACKNOWLEDGEMENT

We thank Li-Ping Sun for useful discussions. This project is supported by the National Natural Science Foundation of China under Grant No. 11261130311.

-
- [1] S.K. Choi *et al.*, Belle Collaboration, Phys. Rev. Lett. **91**, 262001 (2003).
 - [2] B. Aubert *et al.*, BARBAR Collaboration, Phys. Rev. Lett. **95**, 142001 (2005).
 - [3] C.Z. Yuan *et al.*, Belle Collaboration, Phys. Rev. Lett. **99**, 182001 (2007).
 - [4] B. Aubert *et al.*, BARBAR Collaboration, Phys. Rev. Lett. **98**, 212001 (2007).
 - [5] X.L. Wang *et al.*, Belle Collaboration, Phys. Rev. Lett. **99**, 142002 (2007).
 - [6] G.Pakhlova *et al.*, Belle Collaboration, Phys. Rev. Lett. **101**, 172001 (2008).
 - [7] R. Mizuk *et al.*, Belle Collaboration, Phys. Rev. **D78**, 072004 (2008).
 - [8] S.K. Choi *et al.*, Belle Collaboration, Phys. Rev. Lett. **100**, 142001 (2008).
 - [9] K.Chilikin *et al.*, Belle Collaboration, Phys. Rev. **D88**, 074026 (2013).
 - [10] M. Ablikim *et al.*, BESIII Collaboration, Phys. Rev. Lett. **110**, 252001 (2013).
 - [11] Z.Q. Liu *et al.*, Belle Collaboration, Phys. Rev. Lett. **110**, 252002 (2013).
 - [12] T. Xiao, S. Dobbs, A. Tomaradze and Kamal K. Seth, Phys. Lett. **B727**, 366 (2013).
 - [13] M. Ablikim *et al.*, BESIII Collaboration, Phys. Rev. Lett. **111**, 242001 (2013).
 - [14] M. Ablikim *et al.*, BESIII Collaboration, Phys. Rev. Lett. **112**, 132001 (2014).
 - [15] I. Adachi *et al.*, Belle Collaboration, arXiv:1105.4583 [hep-ex]
 - [16] S. L. Zhu, Phys.Lett. B. **625**, 212 (2005).
 - [17] H. Hogaasen, J.M. Richard and P. Sorba, Phys. Rev. **D73**, 054013 (2006).
 - [18] D. Ebert, R.N. Faustov and V.O. Galkin, Phys. Lett. **B634**, 214 (2006).
 - [19] N. Barnea, J. Vijande and A. Valcarce, Phys. Rev. **D73**, 054004 (2006).
 - [20] Y. Cui, X.L. Chen, W.Z. Deng and S.L. Zhu, High Energy Phys. Nucl. Phys. **31**, 7 (2007).
 - [21] R.D. Matheus, S. Narison, M. Nielsen and J.M. Richard, Phys. Rev. **D75**, 014005 (2007).
 - [22] T.W.Chui and T.H. Hsieh, Phys. Lett. **B646**, 95 (2007).
 - [23] L. Zhao, W.Z. Deng and S.L. Zhu, Phys.Rev. **D90**, 094031 (2014).
 - [24] D. Gamermann and E. Oset, Eur. Phys. J. A **33**, 119 (2007).
 - [25] F. E. Close and P.R. Page, Phys. Lett. B **578**, 119 (2004).
 - [26] M. B. Voloshin, Phys. Lett. B **579**, 316 (2004).
 - [27] C. Y. Wong, Phys. Rev. C **69**, 055202 (2004).
 - [28] E. S. Swanson, Phys. Lett. B **588**, 189 (2004).
 - [29] N. A. Törnqvist, Phys. Lett. B **590**, 209 (2004).
 - [30] Y.-R. Liu, M. Oka, M. Takizawa, X. Liu, W.-Z. Deng, and S.-L. Zhu, Phys. Rev. D **82**, 014011 (2010).
 - [31] Ning Li, Shi-Lin Zhu, Phys.Rev. **D86**, 074022 (2012).
 - [32] L. Ma, X.-H. Liu, X. Liu, and S.-L. Zhu, arXiv:1404.3450 [hep-ph].
 - [33] X.-H. Liu, L. Ma, L.-P. Sun, X. L., and S.-L. Zhu, arXiv:1407.3684 [hep-ph].
 - [34] Q. Wang, C. Hanhart and Q. Zhao, arXiv:1303.6355 [hep-ph]
 - [35] F. Aceti, M. Bayar, E. Oset, A. Martinez Torres, K. P. Khemchandani, F. S. Navarra and M. Nielsen, arXiv:1401.8216 [hep-ph]
 - [36] Y.-R.Liu, X.Liu, W.-Z. Deng and S.-L. Zhu, Eur. Phys. J. **C56**, 63 (2008).
 - [37] X.Liu, L.-Z. Gang, Y.-R.Liu, and S.-L. Zhu, Eur. Phys. J. **C61**, 411 (2009).
 - [38] A.E. Bondar, A. Garmash, A.I. Milstein, R. Mizuk and M.B. Voloshin, arXiv:1105.4437 [hep-ph]
 - [39] Z.-F. Sun, J. He, X. Liu, Z.-G. Luo, and S.-L. Zhu, Phys.Rev. **D84**, 054002 (2011).
 - [40] W. Chen, T.G. Steele, M.-L. Du, and S.-L. Zhu, Eur.Phys.J. **C74**, 2773 (2014).
 - [41] J. He, X. Liu, Z.-F. Sun, and S.-L. Zhu, Eur.Phys.J. **C73**, 2635 (2013).
 - [42] Z.-F. Sun, Z.-G. Luo, J. He, X. Liu, and S.-L. Zhu, Chin.Phys. **C36**, 194 (2012).
 - [43] C.D. Deng:2014, J.L. Ping and F. Wang, arXiv:1402.0777 [hep-ph]
 - [44] J. M. Dias, F. S. Navarra, M. Nielsen and C. Zanetti, arXiv:1311.7591s [hep-ph]
 - [45] L. Zhao, L. Ma, and S.-L. Zhu, Phys.Rev. **D89**, 094026 (2014).
 - [46] S. Ahmed *et al.*, (CLEO Collaboration), Phys. Rev. Lett. **87**, 251801 (2001).
 - [47] C. Isola, M. Ladisa, G. Nardulli, and P. Santorelli, Phys. Rev. D **68**, 114001 (2003).
 - [48] C. Isola, M. Ladisa, G. Nardulli, and P. Santorelli, Phys. Rep. **164**, 217 (1988).
 - [49] A. F. Falk and M. E. Luke, Phys. Lett. B **292**, 119 (1992).
 - [50] K. Nakamura, *et al.*, (Particle Data Group), J. Phys. G **37**, 075021 (2010).